Universiteit Utrecht

Cold Atom Nanophotonics Group

Debye Institute

Magneto-Optical Trap Optimization

Author:
Tessa Verboven

Supervisors:
Arjon van Lange, MSc
Dr. Dries van Oosten

June 21, 2013

Contents

1 Introduction

In the Cold Atom Nanophotonics field, interactions between atoms and photons are studied. In the current setup, light is sent through a grid of holes in a golden plate. This creates *surface plasmons*: photon energy that is absorbed in travels along the surface of the plate. The aim of the research is to investigate how cooled atoms interact with these plasmons, when trapping them in the near-field of plasmonic nanostructures.

One of the first steps is to collect a cloud of cold atoms, using a three-dimensional magneto-optical trap. Combining laser cooling with a magnetic field gradient traps the cold atoms. After they are trapped, an optical elevator will move the cloud to the golden plate.

My part was to investigate how the number of atoms the magneto-optical tap loads and the loading can be maximized. This is important, because the atoms have to be moved from the trap to the plasmonic nanostructure. Along the way atoms will be lost. The larger the number of atoms we start out with, the higher the probability there will be enough atoms in the end to perform a good measurement.

We tested the dependence of the loading efficiency for several parameters. To understand this, the theory and setup of a magneto-optical trap is discussed in the next sections.

2 Trapping atoms in a Magneto-Optical Trap

2.1 Definitions

A magneto-optical trap or MOT uses photons and a gradient magnetic field to cool and trap atoms. When working with lasers, certain parameters are frequently used. We will discuss them in the following sections.

2.1.1 Natural linewidth γ

The *spectral linewidth* is the linewidth of a spectral line as seen in the emission spectrum of an atom. But even when the atom is not interacting with a light field, it still has a non-zero linewidth. This is called the *natural linewidth*. We can deduce it using the Heisenberg uncertainty, which states that the uncertainty of a transition ΔE is linked to the lifetime of the excited state:

$$\Delta E \Delta t \gtrapprox \frac{\hbar}{2} \rightarrow \Delta t \gtrapprox \frac{\hbar}{2\Delta E}. \tag{1}$$

The natural linewidth (in Hz) is then

$$\gamma \equiv 1/\tau = 1/\Delta t \lessapprox \frac{2\Delta E}{\hbar}. \tag{2}$$

For this reason the natural linewidth is also called the *decay width* or *decay rate*.

2.1.2 Detuning δ

The detuning is the frequency of a laser beam in terms of distance to the resonance frequency. It is defined as $\delta = \omega_l - \omega_{res}$. A *red-detuned* laser beam has $\delta < 0$, a *blue-detuned* laser beam has $\delta > 0$. Often the detuning is given in terms of the natural linewidth δ/γ.

2.1.3 Saturation parameter s

The saturation parameter gives us the distribution of our population of atoms between the ground state and the excited state. When $s \ll 1$ most of the atoms are in the ground state. When $s \gg 1$ atoms are distributed equally over the ground state and the excited state. The laser excites atoms in the ground state, but also stimulates emission by the excited atoms. For large s the atoms are saturated: the rate at which ground state atoms are excited is equal to the decay rate of the excited atoms.

The expression for s is

$$s \equiv \frac{s_0}{1 + (2\delta/\gamma)^2}. \tag{3}$$

Here s_0 is the on-resonance saturation parameter, $s_0 \equiv I/I_s$, with I the intensity of the laser light and $I_s \equiv \pi hc/3\lambda^3\tau$ the saturation intensity. This is analogous to the ratio of the number of photons causing stimulated emission to the number of photons spontaneously emitted (see section 2.2.1).

2.2 Laser Cooling

To cool atoms, their kinetic energy has to be decreased. To do so, the interaction between atoms and photons are used.

2.2.1 Spontaneous emission

As known from quantum mechanics, atoms have discrete energy states with specific energies. Transitions between these states can involve photons to supply or carry away the difference in energy. There are three types of radiative transitions between these states:

- **Absorption**
  In an absorption event a photon of the laser is absorbed by the atom, adding an energy $\hbar\omega_l$ and bringing it into a higher energy state.
- **Stimulated emission**
  This is the reverse action of absorption. An atom falls back to a lower energy state while emitting a photon into the mode of the light field - with equal energy, polarization, phase and direction of propagation as the other photons of the laser.
- **Spontaneous emission**
  Takes place when an atom falls back to a lower energy state, but instead of emitting a photon into the mode of the field it is emitted in a random direction.

As we will see in the next section, atoms decaying by spontaneous emission will withdraw energy from the system of 'light field + atoms'.

2.2.2 Scattering Force

Maxwell already theoretically derived that electromagnetic radiation can exert pressure on a surface. On atomic level, this is explained by a photon having a certain momentum $\vec{p}_p$ that is absorbed by an atom. By conservation of momentum, the atom adds this $\vec{p}_p$ to its own momentum $\vec{p}_a$. If the atom then decays *spontaneously*, it emits a photon having a momentum $\vec{p}_p$. The direction of the emitted photon is random, resulting in $\langle\vec{p}_e\rangle = 0$.

If the absorbed photons all have velocities in the $\hat{z}$-direction, the net momentum becomes

$$\langle\vec{p}_{net}\rangle = \langle\vec{p}_{abs}\rangle + \langle\vec{p}_{em}\rangle = \langle p_{abs}\rangle\hat{z} + 0. \tag{4}$$

When the photon and atom are travelling in opposite direction, the photon will decrease the momentum of the atom by p_{net}. The result is a net 'push' in the direction of momentum of the photon being absorbed. The force associated with this pressure is called the *scattering* or *dissipative* force. The temperature of the system is lowered, because it depends on the momentum of the atoms by $T = E_k = \frac{\langle p^2\rangle}{2M}$.

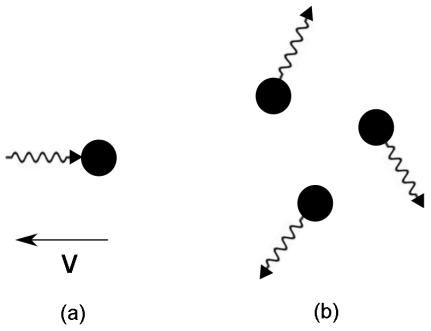

Figure 1: Atoms being decelerated. (a) An atom is excited by absorbing a photon. (b) The atoms decay spontaneously, emitting photons in random directions.

For laser cooling we can explicitly derive the scattering force. In quantum mechanics, the force is the expectation value of the force operator $\mathcal{F}$:

$$F = \langle \mathcal{F} \rangle = \frac{d}{dt}\langle p \rangle = \frac{i}{\hbar}\langle [\mathcal{H}, p] \rangle = \frac{i}{\hbar}\left\langle i\hbar \frac{\partial \mathcal{H}}{\partial z} \right\rangle = -\left\langle \frac{\partial \mathcal{H}}{\partial z} \right\rangle, \tag{5}$$

where $\mathcal{H}$ is the Hamiltonian of the electromagnetic field of the laser. The Ehrenfest theorem is used to calculate $\frac{d}{dt}\langle p \rangle$ and $p = -i\hbar(\partial/\partial z)$ in the (one-dimensional) momentum representation is substitued. After some tough manipulations and approximations of $\mathcal{H}$ (Metcalf & van der Straten, 1999, §3.2) the result for a two-level atom at rest is:

$$F_0 = \hbar k \gamma_p, \tag{6}$$

where $\hbar k$ is the momentum per photon, and

$$\gamma_p = \frac{s_0 \gamma/2}{1 + s_0 + (2\delta/\gamma)^2} \tag{7}$$

is the total scattering rate of light from the laser. The factor $(1+s_0+(2\delta/\gamma)^2)^{-1}$ is the Lorentzian distribution (see section 2.2.3).

When calculating the force for atoms in motion, their speed is treated as a perturbation of atoms at rest. Again using the manipulations for a two-level atom at rest (Metcalf & van der Straten, 1999, §3.3):

$$F \equiv F_0 - \beta v \text{ with } \beta = -\hbar k^2 \frac{4 s_0 (\delta/\gamma)}{(1 + s_0 + (2\delta/\gamma)^2)^2}. \tag{8}$$

The second term compresses the velocity distribution for $\delta < 0$. Because F_0 is always present, the velocity of the atoms is not damped towards a certain value.

2.2.3 Doppler and Power Broadening

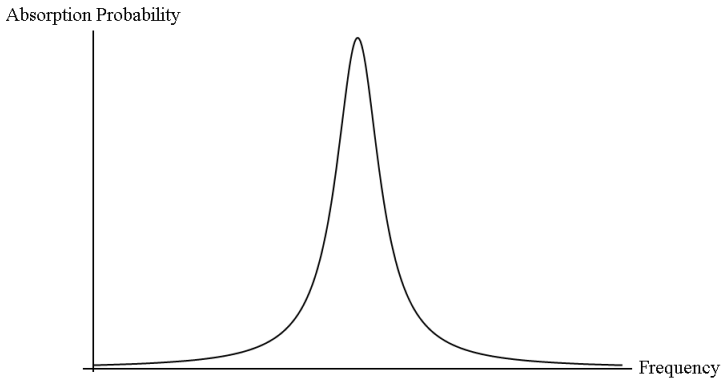

Figure 2: The shape of a Lorentzian.

To push an atom to its excited state, it needs to absorb a photon that has the right frequency. The absorption spectrum for a specific transition is shaped like a Lorentzian $\propto \frac{1}{1+x^2}$ (see Figure 6). The distribution is widened by two effects which will be discussed below.

Doppler broadening
Doppler broadening is caused by the Doppler shift. For atoms with zero velocity, there is a specific photon energy causing a transition to the excited state. Atoms with nonzero velocity observe the frequency of the photons Doppler shifted. A photon with a frequency slightly beneath or above the resonance frequency, can therefore still be absorbed by an atom having the right speed,

$$\omega_{res} \stackrel{!}{=} \omega_p + \omega_D, \tag{9}$$

where ω_p is the photon frequency and ω_D the Doppler shift.

Power broadening
After rewriting (7) to

$$\gamma_p = s_0 \frac{\gamma/2}{\left(1+s_0\right)\left(1+\left(\frac{2\delta}{\gamma(1+s_0)}\right)^2\right)} = \left(\frac{s_0}{1+s_0}\right)\left(\frac{\gamma/2}{1+(2\delta/\gamma')^2}\right) \tag{10}$$

and taking the limit of $s_0 \to \infty$, we see that $\gamma' = \gamma\sqrt{1+s_0} \to \infty$. This is called power broadening, because the intensity of the laser light broadens the linewidth of a transition from $\gamma \to \gamma'$. By definition of the Lorentzian, the full width at half maximum of the absorption spectrum is the power-broadened linewidth γ' of the transition (Metcalf & van der Straten, 1999, equation (3.2)). In Appendix A.1 the results of measuring the absorption spectra for increasing laser intensities are shown, conducted by Citron, Gray, Gabel and Stroud (1977).
When using high laser intensities, $s_0 \gg 1$, the scattering rate saturates to $\gamma_p = \gamma/2$[1]. The scattering force on two-level atoms in rest (6) then becomes $F = \hbar k\gamma/2$.

[1] Using $\lim_{x\to\infty} \frac{x}{1+x} = 1$

2.2.4 Alkali Metal Atoms

Alkali metals are commonly used for laser cooling. Their excitation frequencies are in the visible range, so inexpensive lasers can be used the excite the atoms. Also, the atoms can be vaporized at temperatures in the order of $\sim 10°\text{C}$. Of course a vacuum is needed to make sure the atoms do not collide with gas molecules, which would cause them to gain speed again.
In the sections before, we have worked out a model for laser cooling two-level atoms. In reality, alkali metal atoms are always multileveled and the lasers interact with more than two of them. Usually only the ground and first excited state contribute significantly to the cooling process, but we must remember that the model is an approximation.

When cooling the atoms with a laser, the structure of the energy levels of the atoms is used. As known, an electron can have different values of the total angular momentum quantum number j depending on its orbital angular momentum quantum number l and its spin quantum number s:

$$|l - s| \leq j \leq l + s.$$

The energy levels are structured on two levels:

- **Fine structure**
  The spectral line of an atom consists of closely spaced doublets of energy levels, analogous to the different electron shells (S, P, D). This splitting is caused by the spin-orbit interaction of the electron $\vec{L} \cdot \vec{S}$, where $L = \hbar\sqrt{l(l+1)}$ is the electron orbital angular momentum and $S = \hbar\sqrt{s(s+1)}$ the electron spin. This interaction adds an extra term $H_{SO} \sim \vec{L} \cdot \vec{S}$ to the Hamiltonian, leading to different energies for different $\vec{J}$.

- **Hyperfine structure**
  The energy levels of the fine structure are split into sublevels by interaction between the total angular momentum of the nucleus (or *nuclear spin*) $\vec{I}$ and $\vec{J}$. This adds a term $\sim \vec{I} \cdot \vec{J}$ tot the Hamiltonian, resulting in different energies for different values of the total angular momentum of the atom $\vec{F} = \vec{I} + \vec{J}$. Hyperfine splitting is a much smaller effect than fine splitting.

The fine and hyperfine structure for Rubidium is shown in Appendix A.2.

As for $\vec{J}$ the quantum number associated with $\vec{F}$, m_F, can vary between

$$|I - J| \leq m_F \leq I + J$$

meaning every hyperfine structure level is still $(2I+1)(2J+1)$ degenerate. This degeneracy can be lifted by applying an external magnetic field, causing the *Zeeman effect*. The magnetic field adds an energy depending on m_F, splitting the energy levels.

2.2.5 Saturated Absorption Spectroscopy

To be able to view the spectrum of rubidium, absorption spectroscopy is used (Pal, (n.d)). For this, a laser (the so-called *push* beam) is sent through a rubidium vapor cell at room temperature. This beam is then reflected and sent through the sample again (the so-called *probe* beam). The setup scheme is shown in the figure below.

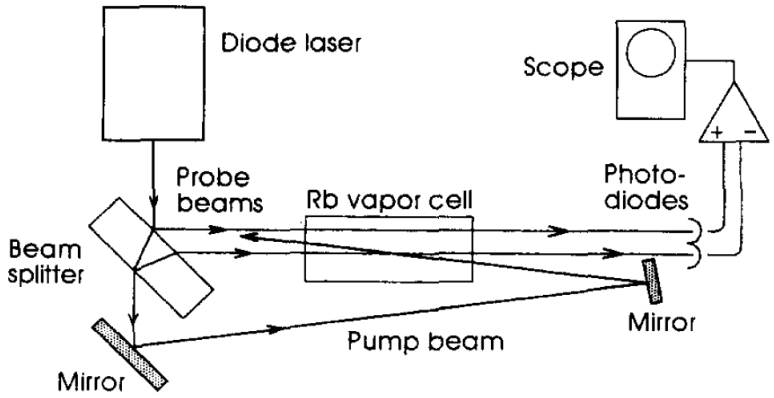

Figure 3: Setup for saturated absorption spectroscopy (Preston, 1996)

Because the laser scans its frequency over the spectrum, atoms will be excited to different hyperfine levels depending on their speed. An atom with $v \sim 0$ in the $F = 2$ state will shift to $F' = 2$ or $F' = 3$ when absorbing a photon[2]. After sending the probe beam through the vapor cell, a photodiode measures its signal. Using an oscilloscope the spectrum of the beam can then be viewed, with time on the horizontal axis and the photodiode current on the vertical axis.
Atoms with nonzero velocity resonate with photons carrying the transition energy. Atoms that are excited by the pump beam, are not in resonance with the probe beam any more. The probe beam spectrum will then show a peak at this frequency because those photons are transmitted.

Some photons have a frequency halfway between transitions, e.g. $F' = 2$ and $F' = 3$. For this frequency an atom can have a certain velocity in the direction of the pump beam, causing it to see the beam redshifted and in resonance with $F' = 2$. Then this atom will see the probe beam blueshifted and in resonance with $F' = 3$. The atom is already in an excited state, and will not be affected by the probe beam. These transmitted photons show up as a peak precisely between the $F' = 2$ and $F' = 3$ peaks. They are called *crossover transitions*. On the next page the result is shown.

[2] F denotes a level in ^2S, F' in ^2P

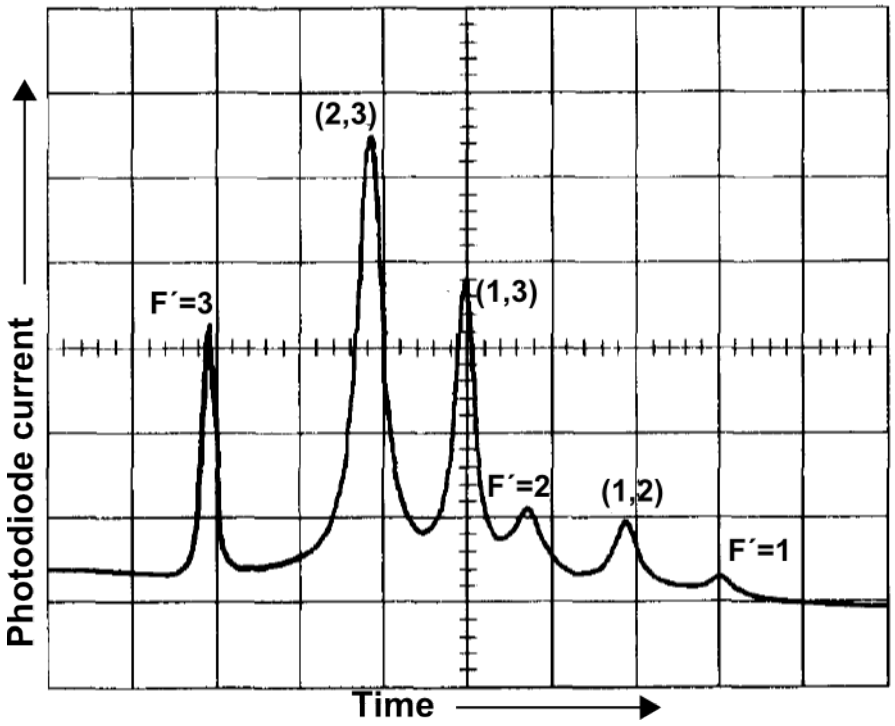

Figure 4: Rubidium spectrum for transitions from the ground state $F = 2$. (A,B) denotes the crossover transitions between $F' = A$ and $F' = B$. (Preston, 1996)

2.2.6 Doppler Cooling

To cool a sample of atoms down, the velocity distribution has to be compressed: the atoms must be decelerated. An atom having a certain velocity can be decelerated by choosing a specific transition in its energy level structure, and then put a laser beam at the transition frequency opposing the direction of motion of the atom. But the atom experiences a Doppler shift, meaning the laser is out of resonance. The atom will see the light blueshifted, so the laser has to be detuned red.
The Doppler shift in electromagnetics for a laser directed along the z-axis and atom with velocity $-v$ along the same axis, is defined as

$$\omega_{lab} = \omega_{atom}\left(1 - \frac{v}{c}\right) \Rightarrow \omega_D = \omega_{lab} - \omega_{atom} = -\frac{v\omega_{atom}}{c}. \tag{11}$$

On the left side, a minus sign was chosen because $\omega_{lab} < \omega_{atom}$ (blueshift).

Using $k = \omega/c$ we see

$$\omega_D = -kv. \tag{12}$$

In general

$$\omega_D = -\vec{k} \cdot \vec{v}, \tag{13}$$

where $k = 2\pi/\lambda$ with λ the wavelength the atom perceives.

The more often an atom absorbs and emits a photon, the more it decelerates. So increasing the scattering rate (which now reads $\gamma_p = \frac{s_0\gamma/2}{1+s_0+[2(\delta+\omega_D)/\gamma]^2}$) by increasing the laser intensity (and by that s_0), maximizes the deceleration

$$\vec{a}_{max} = \frac{\vec{F}_{max}}{m} = \frac{\hbar\vec{k}\gamma}{2M}, \tag{14}$$

using the saturated force derived in 2.2.3.
Beside increasing s_0, having ω_{atom} on resonance maximizes deceleration as well, for the atom then absorbs near the peak of its absorption spectrum and momentum is transmitted optimally. This translates into $\delta + \omega_D \approx 0$. But when the atoms are decelerated their speed decreases, causing ω_D to decrease as well. To keep the requirement above valid δ must be increased by varying either ω_l or ω_{res}.

Sweeping the laser frequency
The detuning increases for increasing laser frequency. As the atoms lose speed, the laser frequency should rise. But at what rate? The acceleration cannot exceed a_{max}. The decrease in ω_D has to be compensated by an increase in δ:

$$\dot{\delta} \approx -\dot{\omega_D} = \vec{k} \cdot \dot{\vec{v}} = \vec{k} \cdot \vec{a} < \vec{k} \cdot \vec{a}_{max} = \frac{\hbar k^2 \gamma}{2M}. \tag{15}$$

Applying a magnetic field to vary the resonance frequency

A Zeeman shift of the resonance frequency occurs when a magnetic field is applied and the Zeeman effect is different for the two levels whose transition is used. The resonance frequency ω_{res} has to decrease with decreasing ω_D. The Zeeman effect is stronger for increasing magnetic fields, so a magnetic field that is maximum near the atom source and then decreases is needed. Slower atoms are only affected by the laser when the magnetic field has become weak enough. Before that point, ω_{res} is too large to be reached by ω_D.

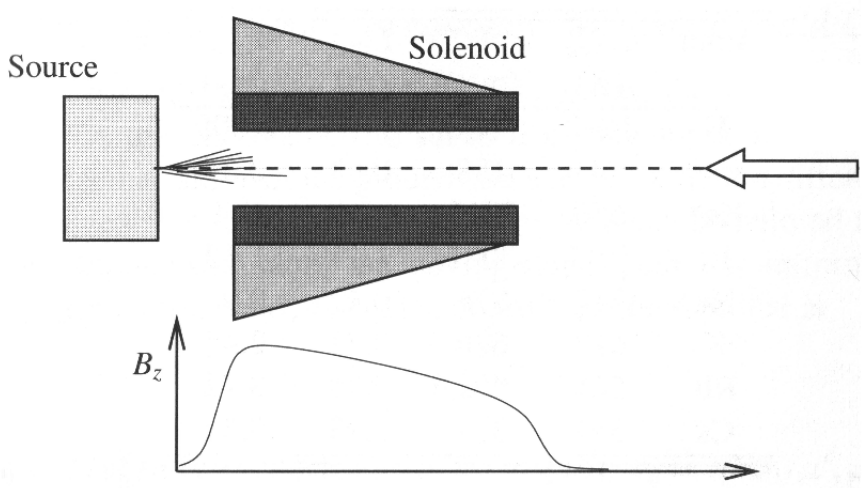

Figure 5: Atoms emerging from the atom soure on the left travel through the solenoid with decreasing diameter opposing the laser beam coming from the right. The generated magnetic field is shown below the scheme. The combination of decreasing Doppler shift (due to decreasing velocity) and a decreasing Zeeman shift, causes the atoms to stay resonant with the photons. (Metcalf & van der Straten (1999), §6.2)

2.3 Laser Trapping

How to decelerate a number of atoms is described in 2.2.6. But they are not decelerated towards any constant value: for $t \to \infty$ all the atoms will be traveling in the direction of the laser beam, pushed by the scattering force.
To prevent this from happening, two counterpropagating laser beams with equal frequencies are set up. An atom moving in line of the beams, will see blueshifted light from the beam it is traveling into (and be excited) but redshifted light from the beam its traveling away from (and not be affected). So all atoms will be decelerated towards zero [3] and stop decelerating when the scattering forces from the two beams are in equilibrium.

2.3.1 Circularly Polarized Light

The way the two counterpropagating beams interact with atoms, is influenced by the polarization. An electromagnetic wave consists of an electric and a magnetic field, oscillating perpendicular to each other. The polarization $\vec{\varepsilon}$ is the superposition of the two fields. The direction of propagation $\vec{k}$ is in the remaining perpendicular direction.
Circular polarization is caused by the electric and magnetic fields being out out of phase by $\frac{1}{4}$ cycle. This causes the polarization to turn in circles, clockwise (σ^-) or counter-clockwise (σ^+) as viewed from the receiver (positive z-axis).

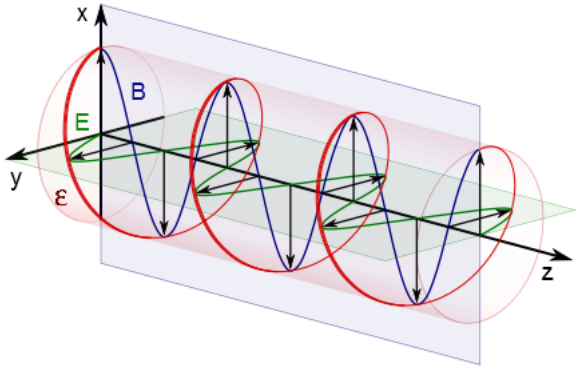

Figure 6: The electric and magnetic fields of σ^+ polarized light.

Two counterpropagating oppositely polarized beams, propagating along the z-axis can be parametrized by

$$\begin{aligned} \sigma^- : \vec{E}^- &= E_0\big(\cos(\omega_l t - kz),\ \sin(\omega_l t - kz),\ 0\big) \\ \sigma^+ : \vec{E}^+ &= E_0\big(\cos(\omega_l t + kz),\ -\sin(\omega_l t + kz),\ 0\big) \end{aligned} \tag{16}$$

The *helicity* of a photon is the projection of spin angular momentum along their direction of propagation (usually the z-axis). It is always equal to $\pm\hbar$ for $\sigma^\pm$ polarized light.

[3] Not to actual zero. T=0 is unphysical: there will always be some thermal motion. See section 2.3.2

The coupling of the light field to atoms depends on the conservation of angular momentum and parity. A photon has nonzero total angular momentum number[4] j with a certain parity. If one applies the parity operator on the angular momentum wave function, all the spatial coordinates are inverted. Even parity means the function is symmetric under that operation, odd parity means it is antisymmetric. For angular momentum the parity is $(-1)^I$ (with I the total quantum number of the atom), so it can be even or odd. This can be accounted for by the shapes of the orbitals of the electron around the nucleus (Ellis, 1999). Using quantum electrodynamics, it can be derived that for each j a photon can have even or odd parity. This results in 'different' electrons: the way they interact with atoms is different (Henley & Garcia, 2007, § 10.4).

An example: a photon with $j = 1$ and odd parity is called the *electric dipole photon*. Before an atom absorbs a photon, the total angular momentum consists of the angular momentum of the atom $\vec{I}_{in}$ and the angular momentum quantum number of the photon j. After absorption, there is only the angular momentum of the atom $\vec{I}_{fin}$. The law of conservation of angular momentum then states[5]

$$\vec{I}_{fin} = \vec{I}_{in} + j \Rightarrow |I_{in} - j| \leq I_{fin} \leq I_{in} + j. \tag{17}$$

This results in the so-called *selection rules*. For our electric dipole photon, we see that $\Delta I \in \{-1, 0, 1\}$. Because parity is a multiplicative quantum number (Henley & Garcia, 2007, § 9.1), for the parity of -1 (odd) to be conserved the initial and final state need to have opposite parity: $I_{in} = \pm 1, I_{fin} = \mp 1 \rightarrow I_{in} * (-1) = I_{fin}$. This is not the case for transitions with $\Delta I = 0$ because those shells are both (anti)symmetric (Ellis, 1999), so only transitions with $\Delta I = \pm 1$ are possible.

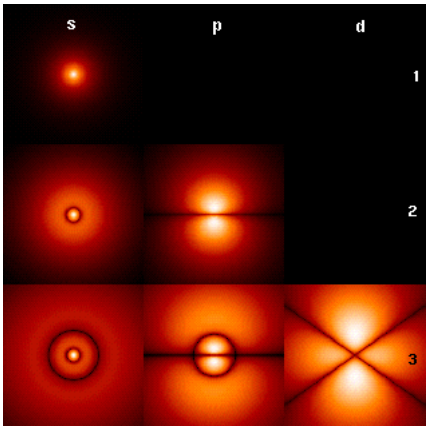

Figure 7: The lowest electron shells for hydrogen. $\Delta I = 0$ corresponds to transitions between S-shells. $\Delta I = \pm 1$ are transitions from S to P or vice versa.

[4]Vectors imply a physical quantity, letters a quantum number

[5]In QM, the total angular momentum of a system $\vec{L} = \vec{I}_1 + \vec{I}_2 + ... + \vec{I}_n$ is quantized. This quantization is characterised by the quantum number L, which can take up values $|I_1 - I_2 - ... - I_n| \leq L \leq I_1 + I_2 + ... + I_n$ (Griffiths, 2005, § 4.3)

For alkali metals, transitions in the hyperfine splitting are used. The same selection rules that apply to absorption - but now for $\Delta F = \{-1, 0, 1\}$ - apply to spontaneous emission as well. Alkali metal ground states have $L = 0$ so $J = L + S = S$. Then $F_g = I + J = I + S$. In accordance with the selection rules described above, a $F_g \rightarrow F_e = F_g + 1$ is used for cooling and trapping. But they have the complication that the excited states can decay to a different ground state $F_g = I - S$ in steps. To solve this a *repump laser* is used, which pumps atoms from $F'_g \rightarrow F'_e = F'_g + 1$, which then decays to the original F_g (see section 3.3.1).

So using the selection rules for circularly polarized light, it is possible to choose a certain transition for cooling and cycle the atoms through by absorbing and spontaneously emitting. As will be described in section 2.4.1, a magnetic field is used to cause a position-dependent shift of the energy levels. This causes atoms right to the trap center to be in resonance with σ^- photons and the atoms left to the trap center with σ^+ photons. Why this shift is necessary will be shown later.

2.3.2 Optical Molasses

When atoms are cooled by three pairs of counterpropagating lasers, but not trapped in a certain point, every atom is decelerated to zero velocity. Because the atoms have different speeds and different starting positions, they do not all end up at the same position. This cooled down, scattered bunch of atoms is called an *optical molasses* (OM).

What temperatures are attainable? There is always some heating due to the recoil of atoms decaying by emitting a photon and absorbing photons. If the recoil velocity is v_r, then the kinetic energy associated with one scattering event is $E_k = 2\hbar\omega_r$: once for absorption and once for decaying. Because the recoil from decay is in a random direction, the atoms obtain recoil velocities in random directions (thermal motion) contributing to the temperature. Calculating E_k when cooling and recoil heating are in equilibrium and minimizing that energy, the Doppler cooling limit is found to be (Metcalf & van der Straten, 1999, §7.2)

$$T_D = \frac{\hbar\gamma}{2k_B} \qquad \text{for } |\delta| = -\gamma/2. \tag{18}$$

This result is derived for a one-dimensional OM with $s_0 \ll 1$ and a two-level atom. However, experiments using 3D OM measure temperatures of $0.1T_D$ (Lett et al., 1988). Apparently the two-level atom picture is inadequate and multilevel theory is needed to explain these temperatures. Experiments have also shown that 3D OM is much less sensitive to alignment errors and perturbations (Lett et al., 1989), making it very suitable for use in the lab.

2.4 Magnetic Trapping

To converge atoms towards a trap center, an inhomogeneous magnetic field can be used. Due to the Zeeman effect, the energy levels will shift proportional to B. And because B varies in space, the shifts will vary as well. Simplified to 1D, the magnetic field is linear and zero in the center. The combination of $\sigma^+\sigma^-$-polarized light and the gradient magnetic field drives atoms to the center $z = 0$ (this will be explained in section 2.4.1).
For a 3D-trap, this gradient field is extended to 3D: the so-called *quadropole field*. It is attained by placing two solenoids on top of each other, and running a current through them in opposite directions (anti-Helmholtz). In the center $B = 0$, so there is no Zeeman shift and the hyperfine levels are degenerate. From there in each direction the magnetic field increases, causing the levels to split and increasing their mutual distance with growing distance from the center.
A 2D-representation is shown in the figure below.

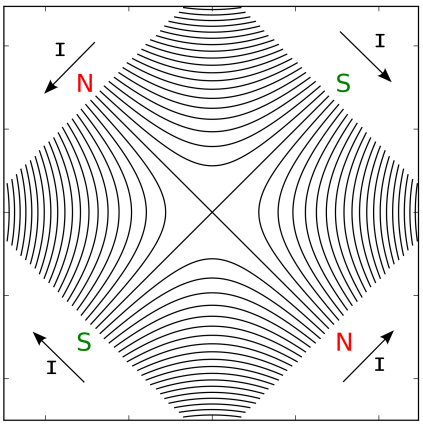

Figure 8: A two-dimensional quadropole field. The arrows indicate the direction of the current through the solenoids, located in the corners of the square. In the center $B = 0$.

2.4.1 Magneto-Optical Trap (MOT)

In a MOT the position-dependent shift caused by B is combined with the selection rules covered in section 2.3.1. Back to the 1D configuration:

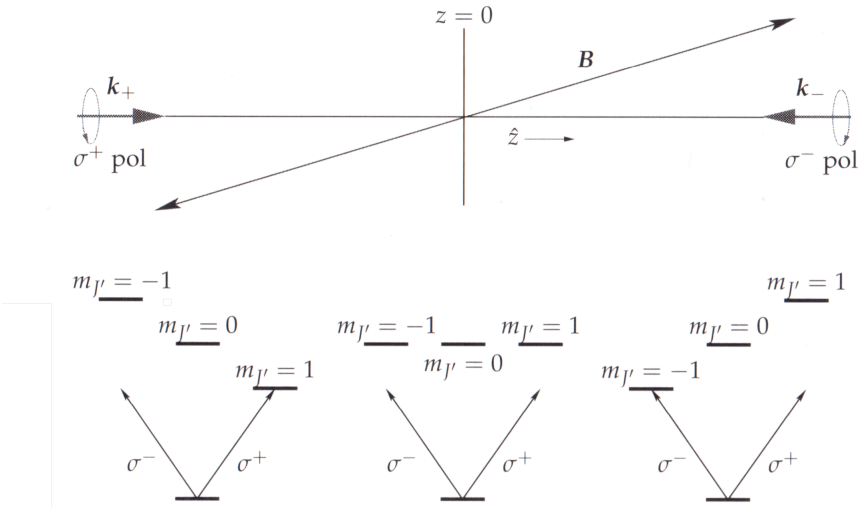

Figure 9: A one-dimensional magnetic field and the shifting of the energy levels it causes.

Both the lasers are detuned $\delta < 0$. Two regimes can be considered: the friction regime $\omega_D \gg \omega_Z$ and the pushing regime $\omega_D \ll \omega_Z$. In the friction regime the motion of the atoms is damped. In the pushing regime the atoms are given a velocity towards the center of the trap.

Consider an atom at position $z > 0$ in the pushing regime with velocity $\vec{v} = v\hat{z}$. Due to the Doppler shift this atom is not in resonance with the beam coming from $z = -\infty$ ($\sigma+$) because it sees it redshifted. The beam coming from $z = +\infty$ is blueshifted and thus closer to resonance. The Zeeman effect causes the level at $\Delta F = +1$ to be shifted upwards, even further away from resonance with σ^+. But the level at $\Delta F = -1$ is shifted downwards, closer to resonance with σ^-. In time, with increasing z, the level moves down more until it is in resonance with the laser. The atom absorbs a photon (and its momentum), and decays after some time. Its velocity has now decreased so the Doppler shift is smaller, but it is still moving in the $\hat{z}$-direction: the magnetic field is still increasing and the energy level keeps lowering, until it hits resonance again. This continues until the atom has zero velocity.

Now there is no Doppler shift but the level is shifted such that the σ^--beam is in resonance even without. The atom starts moving in the $-\hat{z}$-direction and seeing the beam more red. At the same time the energy level moves upwards, until the atom is out of resonance. It then moves into the friction regime, where the beam coming van $z = -\infty$ resonates with the atom. It damps its movement, slowing the atom down to $v = 0$ at the center.

The direction of the magnetic field lines only matters for the direction of the Zeeman shift (up or down) corresponding to the direction of the laser beams. The procedure is symmetric for atoms with a velocity $\vec{v} = -v\hat{z}$. Generalizing to 3D, a system that cools and traps a sample of atoms in three dimensions is obtained.

Accounting for the Zeeman shift in the radiative force gives

$$\vec{F}_{\pm} = \pm\frac{\hbar\vec{k}\gamma}{2}\frac{s_0}{1 + s_0 + \left[2(\delta \mp \omega_D \pm \omega_Z)/\gamma\right]^2} \text{ with } \omega_D = \vec{k}\cdot\vec{v},\ \omega_Z \sim B. \quad (19)$$

Although it is desirable to maximize the atom density in the trap, this is limited. At a certain density, the photons emitted by certain atoms are absorbed by others causing the momentum to be passed on from one atom to another. Also, a dense MOT has a higher collision rate which causes the sample to expand again.

3 Setup

The alkali metal to be cooled is rubidium. An ampul of 1 g natural rubidium is used, consisting of 72.17% $^{85}_{37}$Rb and 27.83% $^{87}_{37}$Rb. Its natural linewidth is $\gamma = 6$ MHz. In this experiment only the $^{87}_{37}$Rb atoms will be cooled. It is vaporized by heating the ampul to a temperature above the melting point $\sim 40°$C. The cooling transition used is 780 nm (section 3.3.1), a wavelength that is relatively easily produced by diode lasers.

After vaporization the atoms are loaded into a 2D MOT, where a two-dimensional quadropole field is present. The atom cloud is then collimated in two dimensions, leaving a horizontal strip of atoms. The 'push' laser beam pushes the atoms to the 3D MOT, where the atoms are trapped and cooled. A drawing of the path the atoms follow through the MOTs is shown below.

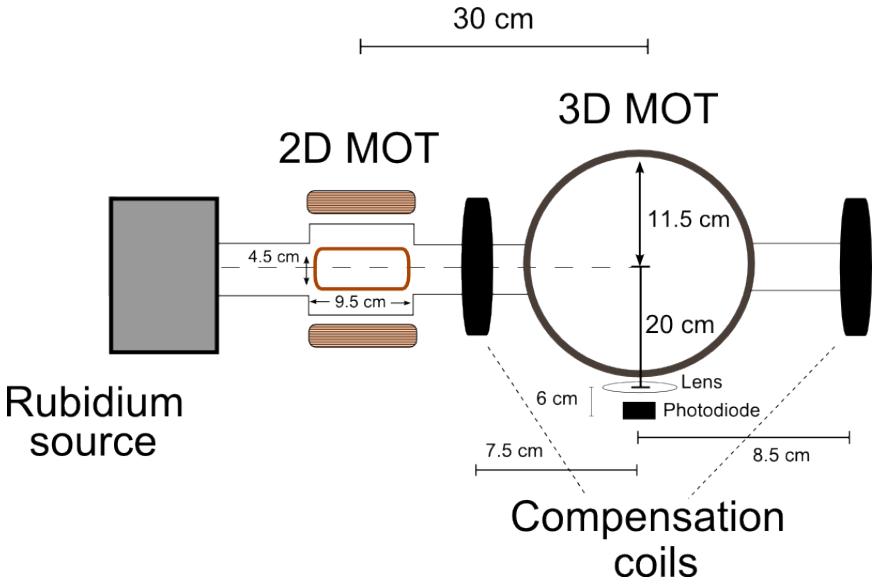

Figure 10: A sketch of the top view of the setup, with rough distances and diameters.

3.1 Vacuum chamber

To create a vacuum in the MOTs chambers, first the pressure is lowered by a prepump and turbopump. Then ion pumps are used to lower the pressure to 10^{-7} mbar in the 2D MOT and 10^{-10} mbar in the 3D MOT.

Ion pump
An ion pump consists of two negatively charged plates in a steel chamber. At low pressure this acts like a cathode. Electrons emitted from this cathode move through the chamber ionizing the particles that are present. The positively charged nucleus is accelerated towards the plates and the electron goes about to ionize more particles (Schulz, 1999).

Differential pump section
The differential pump section maintains the pressure difference between the two MOTs. The pressure in the 2D MOT is higher. The differential pump section consists of a metal cylinder with a tiny hole in it. Atoms with a velocity aligned along the horizontal axis, can travel through the pump section to the 3D MOT. The tube of atoms needs to be well aligned with the cylinder hole to ensure a good transit.

3.2 Diode lasers

Diode lasers consist of semiconductor material in which electrons are excited by a current. If one electron falls back to its ground state, it emits a photon. This photon stimulates emission by the other excited electrons. Many photons are emitted, creating a linearly polarized beam with a Doppler broadened spectrum. It scans around $\lambda = 780$ nm by much less than 1% and has an intensity of ~ 100 mW.

After leaving the diode laser, the beams are locked using saturated absorption spectroscopy (see section 2.2.5). We discuss this in section 3.3.2.

3.2.1 Changing the polarization

The repump lasers are locked with the same method as the reference lasers. Now all the lasers are locked but their polarization is linear. To change the polarization of the cooling and repump beams, $\lambda/4$-waveplates are used. These consist of a material which has different indices of refraction for the different electric field components of the light. By turning the plate n can be varied and the different polarization components can therefore phase-shifted by $\pi/2$ or $\lambda/4$. Because circular polarization requires a phase difference of $\frac{1}{4}$ cycle, the light is now circularly polarized. To know what polarization the light has, a polarizing beamsplitter cube is used. This cube reflects light of one polarization and transmits light of the other polarization. It is not important to know which polarization a beam has; all we need to make sure is that opposing beams in the MOTs have *opposite* polarization.

3.3 Laser Light

To cool and trap the atoms we create six different types of laser beams:

- **2D & 3D MOT cool**
  Laser used for the cycling transition. Tuned slightly below the cooling transition to correct for the Doppler shift.
- **2D & 3D MOT repump**
  Repumps atoms to the original ground state when atoms decay to the wrong ground state after being excited by the cooling laser.
- **Reference beam**
  Used as reference for the cooling lasers to cause a detuning.
- **Push beam**
  Pushes the atoms from the 2D MOT to the 3D MOT through a tube.

Diode lasers produce the first five beams. A part of the reference beam is split off and modulated to the push beam frequency.

3.3.1 Rubidium

The transitions used are all from the ^2S and ^2P levels of the fine structure. The hyperfine structures of these levels are used to lock the lasers. In the hyperfine structure the used transitions are:

- **Reference beam**: Crossover transition (1,3)
- **Push beam** : $F = 2 \rightarrow F' = 3$
- **2D & 3D MOT cool**: Slightly red detuned from $F = 2 \rightarrow F' = 3$
- **2D & 3D MOT repump**: $F = 1 \rightarrow F' = 2$

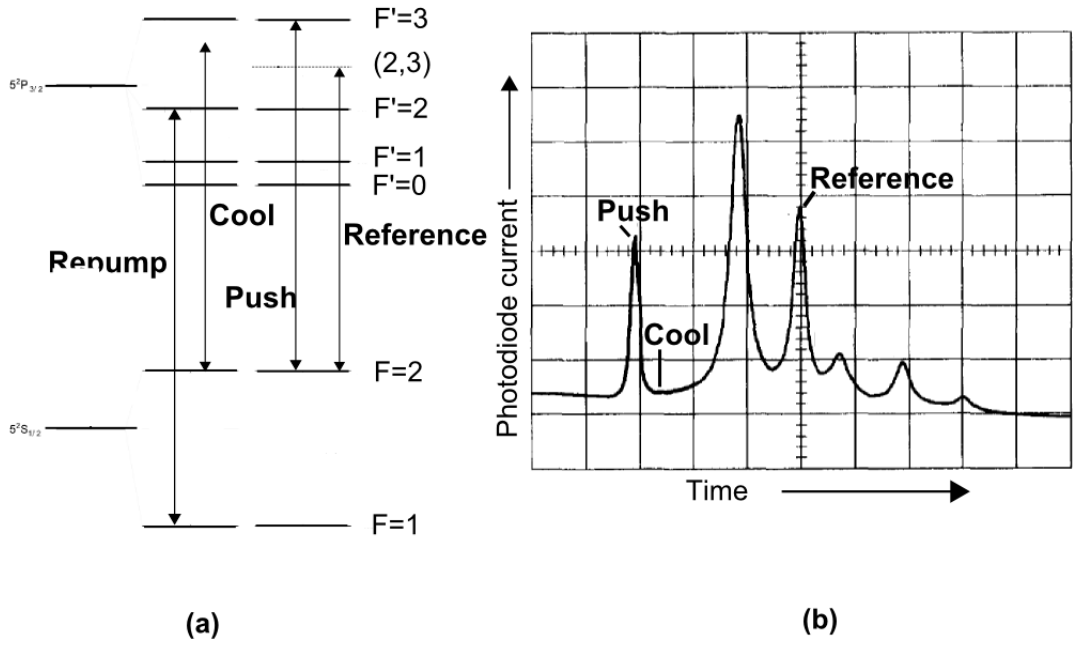

Figure 11: The transitions used for the lasers. (a) In the structure scheme for energy levels. (b) In the spectrum resulting from saturated absorption spectroscopy (see Figure 6.

3.3.2 Laser Locking

Now the transitions are known and visible, the lasers can be locked on specific frequencies. The reference laser has to be locked on the peak of the (1,3) crossover. If there is a small perturbation causing the lock to 'slide' off the peak, it will notice the signal strength becoming weaker but it cannot know if it has fallen to the left or right. This way the laser is not able to correct these perturbations. Therefore, an error signal is used. An error signal is similar to the derivative of the initial signal: it shows steep slopes at the frequencies at which the inital signal has peaks. When we lock on this slope and the frequency is perturbed, the signal strength is increased when the frequency gets smaller, and decreased when the frequency gets bigger. The laser can differ between the two directions of perturbation and is thus able to correct for them. The initial signal and the error signal are shown on the oscilloscope to be able to find the right peak and the corresponding slope.

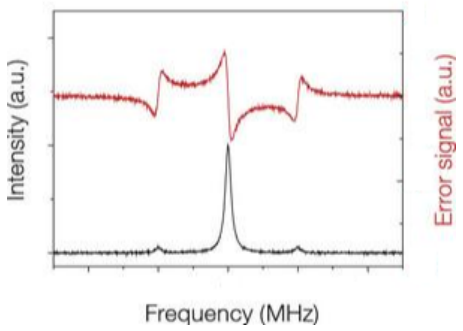

Figure 12: An example of an error signal.

Locking on a peak
After the reference laser is locked, part of the beam is split off and used to create the push beam. The frequency of the beam needs to be shifted from the (1,3) transition to $F' = 3$. Two Acousto-Optical Modulators (AOMs) are used for this. An AOM consists of a vibrating crystal. The vibrations are acoustic waves which diffract the laser beam when it is sent through. When a photon absorbs the energy of the acoustic wave its energy can be changed. After diffraction the different orders have different frequencies. The order with the desired frequency can be filtered out by blocking the other orders. This way the frequency of the beam can be changed.

The AOMs motivate the choice for the reference beam to be locked on the (1,3) peak: they modulate the beam by approximately 100 MHz. The difference between (1,3) and $F' = 3$ transition is $79 + 133 = 212$ MHz (Steck, 2001). So two AOMs can modulate the beam to the desired frequency.

Offset locking

The cooling lasers cannot be locked on a transition peak, because we want them detuned. This is why the reference beam is needed. Each of the cooling lasers is mixed with the locked reference beam. The mixed signal is then split into two paths which are sent through cables with different length which causes a phase difference between them. When the signals are mixed again after, an interference pattern shows.

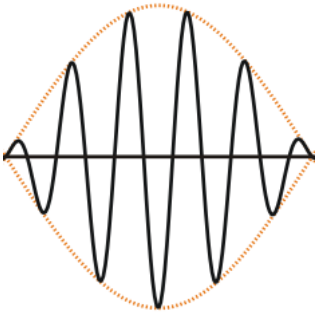

Figure 13: An example of a beat note, as the interference pattern would be.

Showing the probe beam signal with the interference pattern on the oscilloscope, a downward slope beside the $F' = 3$ peak is chosen to lock on. After locking, a Direct Digital Synthesizer (DDS) can be used to change the phase difference (identical to changing the length of one of the two cables used to create the phase difference) which broadens or narrows the interference signal. This changes the 'positions' of the slopes, thus changing the frequency the laser is locked on.
The oscilloscope signal cannot tell us what the desired detuning is. The DDS is used to change the detuning afterwards by maximizing the fluorescence of MOT.

The repump lasers are locked with the same method as the reference lasers. The repump and cooling beams are mixed on the laser table and sent to the MOTs through a fiber. On the MOT table the beams are split once again and aligned in pairs of opposite polarization, in directions perpendicular to each other.

3.4 Magnetic Field

The 2D MOT has a quadropole magnetic field in the x, y-plane. This is created by using four rounded rectangular solenoids with 9 windings (see figure 8). One power source is used for all the magnets which are connected in series. The used current varies from $1 - 5$ A. The $^{87}_{37}$Rb atoms are trapped in the x, y-plane leaving a long strip of atoms along the z-axis (horizontal). The $^{85}_{37}$Rb atoms are unaffected by the 2D trapping system even though they are present. The push beam pushes the $^{87}_{37}$Rb atoms through the tube towards the 3D MOT, leaving most of the $^{85}_{37}$Rb atoms behind.

As described in section 2.4.1 the 3D quadropole magnetic field is created by two coils in anti-Helmholtz configuration. Each of the coils have 180 windings. Again, the two coils are connected in series. The current varies from $5 - 15$ A and the resistance of the circuit is about 1.5 Ω. Because the coils are big and have a large current, they are watercooled. This causes their temperature to rise more slowly.

After installing the 2 fields, it turned out the 3D magnetic field disturbed the 2D field which caused misalignment of the atom strip and the tube. To solve this a compensation coil was placed between the 2D and 3D MOTs with 320 windings and a diameter of 34 cm. This corrected the disturbance of the 2D field, but also changed the 3D field. So another compensation coil was placed on the opposite side of the 3D MOT to compensate the effects of the first compensation coil. Due to parts of the chamber blocking the space, the distance could not be the same for the two coils. Therefore, the diameter is smaller (20 cm) to keep the magnetic field strength equal. These two coils are connected in series as well, with currents of $1-3$ A and a total resistance of approximately 20 Ω.

The compensation coils need to be calibrated to the 3D coils. The currents of the 3D coils are varied from 1 - 20 A, corresponding to 0.1 - 3 A for the compensation coils. The results are shown in Appendix B.1. Although with an uncertainty in reading off the values of 0.09 A the fit is quite accurate, the data points clearly show some steps (e.g. at $I \in \{0.5, 1.0, 1.5, 2.1, 3.0\}$ A). Manually controlling the power supply thus falls short, because we are interested in steps smaller than 0.1 A for the compensation coils.

The direction of the current and the configuration of the polarized beams have to be in accordance (the σ^+-beam needs to enter at the side where $B < 0$, see section 2.4.1). However, we do not need te know which laser beam has which polarisation. If the MOT is not working because the direction of the magnetic field is incorrect, it is easily solved by reversing the direction of the current.

3.4.1 Switching

For certain measurements it would be useful to construct several loaded MOTs after eachother, by switching the magnets on and off (preferably computer controlled). Doing so means we have to take into account the self-induction of the magnets, for it can cause peak voltages and slowly decaying currents. A switch based on an insulated gate bipolar transistor (IGBT (Sattar, 2003)) is used for this.

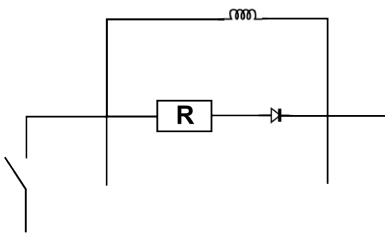

Figure 14: A switching circuit.

By switching the coils off, a back emf is created (using $\varepsilon = V = RI$)

$$\varepsilon = -L\frac{dI}{dt} \rightarrow I(t) = I_0 e^{-t/\tau} \text{ with } \tau = L/R \tag{20}$$

where L is the inductance of the coils in Henry (Griffiths, 1999). The current decreases to zero in the switch circuit instead of in the coils. This way the magnetic field can be turned off in τ seconds. The switches used can handle voltage peaks of maximally 1200 V. By varying the resistance in the switch circuit, the characteristic decay time τ can be controlled. Ideally, we want these to be of the same order for all three coil circuits. The inductances L have been calculated, by measuring the decay time with the resistors already present. To relieve the coils a characteristic decay time of approximately ~ 1 ms was chosen. With the available resistors the following switch resistances, voltage peaks and decay times were achieved:

Switches	L (mH)	R (Ω)	ΔV (V)	τ (ms)
2D coils	4	5.5	20	0.3
3D coils	30	9.7	100	3
Compensation coils	50	49.7	150	1

It is clear to see that the voltage peaks are all far below the limit of the switches of 1200 V. The characteristic times of the 3D MOT and compensation coils are in the intended order, but the 2D MOT current decays very fast. This is no problem: in the experiments done the 2D switch is not yet used. Furthermore, a large τ was mainly meant to make sure the 3D coils would not be burdened too heavily. Having a smaller time for the 2D coils causes no problems.

With this setup, we are able to trap atoms for a specific time. By placing a lens and a photodiode in front of a glass window the fluorescence and hence efficiency of the MOT can be measured.

4 Results

4.1 Number of atoms

The number of atoms trapped by the MOT can be found by looking at the fluorescence of the atom cloud. The fluorescence depends on the decay rate γ_p and the detuning δ of the laser beams. The decay rate saturates to $\gamma/2$ for high intensities, which is the case in this experiment (see section 2.2.3). The detuning dependence arises from the absorption efficiency of the atoms. The atoms are cooled, so they have low velocities. Therefore they will absorb the laser photons most efficiently when the laser frequency is on resonance. A larger detuning causes less photon absorption, followed by less photon emission by the atoms. This absorption spectrum is shaped like a Lorentzian, as described in section 2.2.3. So for a specific detuning the number of photons emitted by the atoms is

$$N_p = \mathcal{L}(\delta)\ \gamma_p\ t_{exp}\ N_a, \tag{21}$$

where $\mathcal{L}$ is the Lorentzian and t_{exp} exposure time of the photodiode.

The photodiode collects photons emitted by the sample with a responsivity of $\eta = 0.52 \pm 0.2$ A/W (see the User's Guide, §6.1 at 780 nm). We set the photodiode to the 40 dB setting and install it in a circuit with 50 Ω resistor. It then has a gain of $\zeta = 0.75 \cdot 10^5 \pm 2\%$ V/A (see User's Guide, chapter 6 at the 40 dB setting). The power of the photons that hit the photodiode in Watt is

$$P = \frac{I}{\eta} = \frac{V}{\eta\zeta} = 2.6 \cdot 10^{-5} \times V \tag{22}$$

with an uncertainty of less than 0.01 %. Dividing this by the energy of a photon with resonance frequency, $E_p = \frac{hc}{\lambda} = 7.4 \cdot 10^{-18} J$ using $\lambda = 780$ nm, is the number of photons intercepted by the photodiode:

$$N_{p,PD}/t_{exp} = \frac{P}{E_p} = 3.5 \cdot 10^{12} \times V. \tag{23}$$

These are only part of the total number of photons emitted, namely the fraction of the spherical shell that is measured by the photodiode: $\Delta\Omega/4\pi$ where $\Delta\Omega$ is the solid angle. The photodiode measures the photons that reach the lens. The lens is 7.62 cm in diameter. If we approximate the lens as a two-dimensional circle, the area is $A_{lens} = \pi * 7.62 \cdot 10^{-2} \sim 4.5 \cdot 10^{-3}$ m^2. The distance from the lens to the center of the MOT is roughly 20 ±2.5% cm. The spherical shell the lens is located on thus has a surface area of $A_{shell} = 4\pi R^2 = 4\pi(20 \cdot 10^(-2))^2 \sim 0.50 \pm 5\%$ m^2. The total number of photons the cloud emits becomes:

$$N_p/t_{exp} = \frac{A_{shell}}{A_{lens}} N_{p,PD} = 9.0 \cdot 10^3 \times 3.5 \cdot 10^{12} \times V = 31.5 \cdot 10^{15} \pm 5\% \times V. \tag{24}$$

These two equations can be combined to give the number of atoms. Using $\gamma_p \to \gamma/2$ for $s_0 \gg 1$,

$$N_{atoms} = \frac{N_p/t_{exp}}{\mathcal{L}(\delta)\ \gamma/2} = \frac{2 \times 31.5 \cdot 10^{15} \times V}{\mathcal{L}(\delta) \times 6 \cdot 10^6} = \frac{5.25 \cdot 10^{11} \pm 5\% \times V}{\mathcal{L}(\delta)} \tag{25}$$

with $\mathcal{L}(\delta) = s_0(1 + s_0 + (2\delta/\gamma)^2)^{-1}$ (Steck, 2001, §4.3.4).

To use this equation, it is necessary to determine s_0. Knowing the fluorescence spectrum (with fluorescence on the vertical axis and detuning on the horizontal axis) is a Lorentzian, we measure the fluorescence for several detunings and fit a Lorentzian shape to the data. To normalize - only the ratio to maximum fluorescence is important - two different methods are used:

(a) The MOT is loaded at a certain detuning δ/γ and then swept to resonance. The normalized Lorentzian is the ratio of the fluorescence after loading to the fluorescence peak at resonance.

(b) The MOT is loaded maximally and then swept to a certain detuning. The normalized Lorentzian is the ratio of the fluorescence at that detuning to the fluorescence peak the curve would have had if we had swept to resonance.

The cooling laser frequencies of the 2D and 3D MOTs can be computer controlled using the DDS. Before starting the experiments, the resonance detuning is determined by looking at the cloud with a camera. The laser frequency is increased from a red detuning until no atoms are loaded in the MOT, but there is a faint cloud visible. The atoms are not loading because the lasers are not red detuned and are thus not seen by atoms with nonzero velocity. But atoms with zero velocity are cycling the cooling transition and emitting light. This was the case for $\Delta f_{2D,res} \approx 195$ MHz and $\Delta f_{3D,res} \approx 212$ MHz[6]. The photodiode signal is sent to a computer using a National Instruments Card.

[6]The corresponding DDS frequencies are $f_{2D} = 51$ MHz and $f_{3D} = 65$ MHz.

4.1.1 Sweeping to resonance

All the detunings mentioned in this section can calculated from the DDS frequency by $\delta = (f_{DDS} - f_{DDS,res})/\gamma$. The exposure time is $t_{exp} = 11\ s$ and the sampling rate $\nu = 10.000$ Hz. The coils are switched on for the first 10 seconds, and off for the last second. The 2D MOT lasers are set to $\delta_{2D} = -0.5\gamma$ MHz. The 3D MOT lasers are set to four consecutive frequencies:

i) The detuning $\delta_{3D,1}$ that is being varied, loading the MOT for almost 10 seconds. After approximately 7 seconds the loading curve flattens to a constant fluorescence.

ii) The DDS triggers the laser to sweep to resonance $\delta_{3D,2} = 0$ after approximately 9.95 seconds. 10 ms after the trigger the fluorescence starts to increase[7] and shows a peak in the photodiode signal.

iii) 50 ms after the resonance trigger, the DDS triggers the lasers to $\delta_{3D,3} \gg \gamma$. 10 ms later the fluorescence drops. In the blue regime atoms do not see the laser. The magnets are turned off some time after. This part of the curve will be used as a background measurement.

iv) The DDS triggers the laser to a frequency $\delta_{3D,4}$ just below resonance after approximately 10.5 seconds. If the frequency jump when starting a new measurement is too large, the lasers jump out of lock.

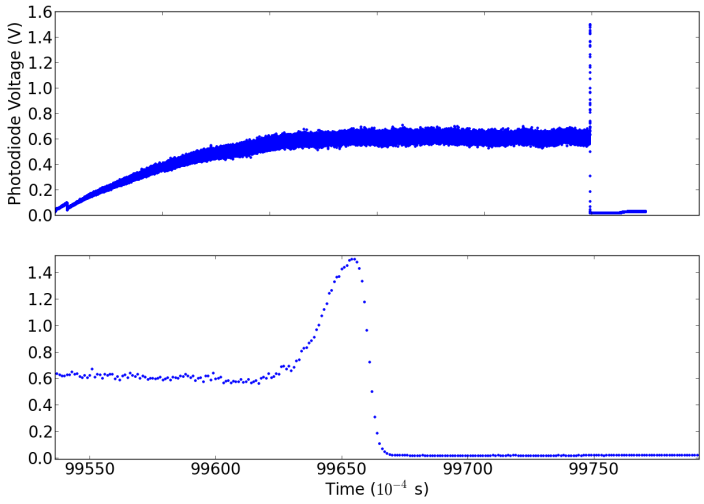

Figure 15: The loading curve for $\delta = -3.3\gamma$. The complete loading curve is shown above. The lower graph zooms in on a sweep from a certain detuning to the resonance frequency (the peak), after which the laser is swept far over resonance (drop in fluorescence to nearly zero.

[7] The primary objective was to let the lasers 'step' to the next frequency, but it turned out the lasers were not able to follow the DDS that fast.

The exact timing of the triggers is not the same for each measurement because it is done manually. Eight measurements were performed, for detunings $\delta \in \{-5.8, -5.0, -4.2, -3.3, -2.5, -1.7, -0.8, 0\}\gamma$. See Appendix C.1. As can be seen from the graphs, at detunings -5.8γ and -5.0γ the fluorescence is no more than 0.5 V. This means the atoms are not loading into the MOT, and these measurements are unreliable. The last measurement, at detuning 0, shows no signs of loading as well. These three will not be used as fitting data.

By averaging the data points in the interval of [9.0, 9.9] seconds, the loading fluorescence V_l in Volt is obtained. This is divided by the maximum value in the time interval [9.9, 10.0] seconds, which is the peak fluorescence V_p. The background fluorescence V_b is the average of the data points in the time interval [10.2, 10.4] seconds. Then

$$\mathcal{L}_{(a)}(\delta = a\gamma) = \frac{V_l - V_b}{V_p - V_b} \tag{26}$$

gives the value of the Lorentzian for a certain detuning $a\gamma$, with $a \in \{-4.2, -3.3, -2.5, -1.7, -0.8\}$. Fitting a Lorentzian shape through these data points gives $s_0 = 28.7$. See figure 4.1.1 on the next page.

The error bars shown are the standard deviations of each data point, calculated using $\sqrt{\frac{x_1^2+x_2^3+\ldots+x_n^2}{n}}$. They show the spread in the used data points. As one can see, the error is larger for higher detunings. Referring back to the loading curves in Appendix C.1, this is caused by the wider spread of data in the loading regime. The fluctuations in the fluorescence of the MOT become higher when it contains a larger number of atoms. Now considering the reliability of the fit, it is clear the accuracy is good. It is well within the marges of lower detunings, and just within for the higher detunings.

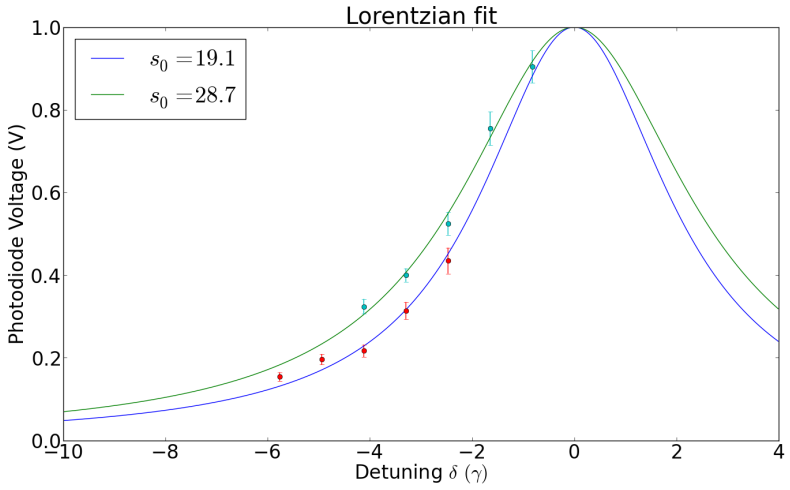

Figure 16: The data points and fits for measurements methods (a) and (b).

4.1.2 Maximally loading

To obtain better data points for high detunings, the MOT is loaded maximally and then swept to lower frequencies. The result of measurement (a) shows the Lorentzian is steepest at approximately 2γ detuning. A detuning of -1.7γ is therefore chosen as reference for maximally loading.
First the reference measurement is made for $\delta_{3D,1} = -1.7\gamma$. Then five measurements are done where $\delta_{3D,1} = -1.7\gamma$, $\delta_{3D,2} = b\gamma$ with $b \in \{-5.8, -5.0, -4.2, -3.3, -2.5\}$, $\delta_{3D,3} = 0$ and $\delta_{3D,4} \gg \gamma$. Again $\delta_{2D} = -0.5\gamma$. See Appendix C.2.

It is not possible to sweep to resonance and to a higher detuning in one measurement, because the lasers would jump out of lock. As can be seen from the loading curves, the MOT does not load the same amount of atoms each measurement. This would result in different resonance peaks. Assuming the ratio between loading and peak is constant for a certain detuning, the "would-be" peak for each measurement can be calculated. Using the reference measurement, this ratio is

$$\alpha = \frac{V_{p,ref}}{V_{l,ref}} \tag{27}$$

where $V_{p,ref}$ is the maximum value in time interval [9.9, 10] seconds and $V_{l,ref}$ the average of data points in time interval [9.8, 9.9] seconds. When we multiply V_l, the loading fluorescence for the measurements with detunings b which is obtained by averaging the data points in time interval [9.8, 9.9] seconds, by this ratio the peaks these loading curves would have had are acquired:

$$V_p = \alpha V_l. \tag{28}$$

The fluorescence V_m (m for minimum) measured after the sweeping the laser to higher detunings b, is the fluorescence the MOT would have had at

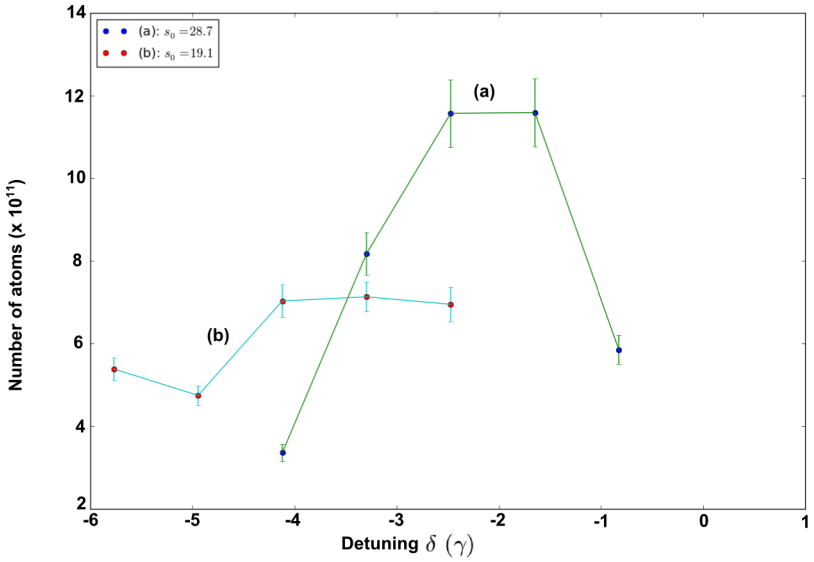

Figure 17: The number of atoms using the fluorescence and saturization parameters found in methods (a) and (b). The right detuning can increase the number of atoms by a factor 2 or 3.

those detunings if it were able to load properly. This is the analoque of V_l in method (a). It is the minimum value in time interval [9.9, 10] seconds. The background is the average of data points in time interval [11.7, 11.9] seconds. The Lorentzian value now is

$$\mathcal{L}_{(b)}(\delta = b\gamma) = \frac{V_m - V_b}{V_p - V_b}. \tag{29}$$

The line fitted through these values is shown in figure 4.1.1, giving $s_0 = 19.1$. The error bars were calculated analogous to method (a). Again, the error bars are smaller for higher detunings. The fit is within the error bars for the lowest three detunings. Despite the lower accuracy of the fit for the highest two detunings, it is evident that $\mathcal{L} \to 0$ for $\delta \to \infty$ as desired.

The two different methods return on-resonance saturation parameters in the order of ~ 10. The estimated value was 60 corresponding to this result.

Now we are able to calculate the number of atoms, using equation 25. Here, we plug in the values for s_0 we found in the paragraphs above and the fluorescence the MOT gives at a certain detuning (V_l for method (a) and V_m for method (b)). See Figure 17 on the next page.

4.2 Optimizing

The efficiency of the MOTs depends on many parameters. To optimize its performance we tune the following:

- **Alignment**
  For optimal trapping and cooling, it is preferred the three pairs of laser beams cross in one point. Also, two opposing laser beams need to be antiparallel as exact as possible. This can be varied by tuning the lenses and mirrors used to focus the laser beams. Finally, the push beam needs to be aligned with the tube connecting the 2D and 3D MOT.

- **Current of the 2D magnets**
  The atoms in the 2D MOT have to be squeezed together tightly to make sure they fit through the tube leading them to the 3D MOT. But more important is that the strip of atoms is well aligned with this tube. If the magnetic field is too weak, the tube will be too thick. If it is too strong, the magnetic field will pull the strip skew (because setting up a magnetic field with a perfectly aligned center is only theoretically possible). A balance needs to be found between these two extremes.

- **Current of the 3D magnets**
  A stronger field means a stronger trap, which is desirable. But when the atoms are squeezed more tightly, the probability an atom absorbs a photon just emitted by another decaying atom grows. This event does not contribute to cooling the atoms and is therefore unwanted. Again, a balance needs to be achieved.
  When varying the current of the 3D MOT, the current of the compensation coils have to be adjusted as well.

- **Current of the compensation coils**
  A specific current of the 3D magnets requires a certain compensation coils current. We tune this current independently of the 3D current to see in what way it boosts the efficiency of the MOT. Also, a rough calibration to the 3D coils current will be made.

- **Intensity of the push beam**
  A stronger push beam emits more photons per time unit, causing more collisions with atoms. More atoms will be pushed through the tube. However, if the atoms are pushed too firm they are scattered in all directions. There is a certain intensity which optimizes these effects.

- **Intensity of the 2D and 3D cooling and repump beams**
  Intensifying these beams causes more collisions between photons and atoms: the atoms will be cooled faster. It is expected that a higher intensity will increase the fluorescence of the MOT.

- **Varying the detuning of the 2D and 3D cooling beams**
  There is a certain detuning for which the atoms resonate best.

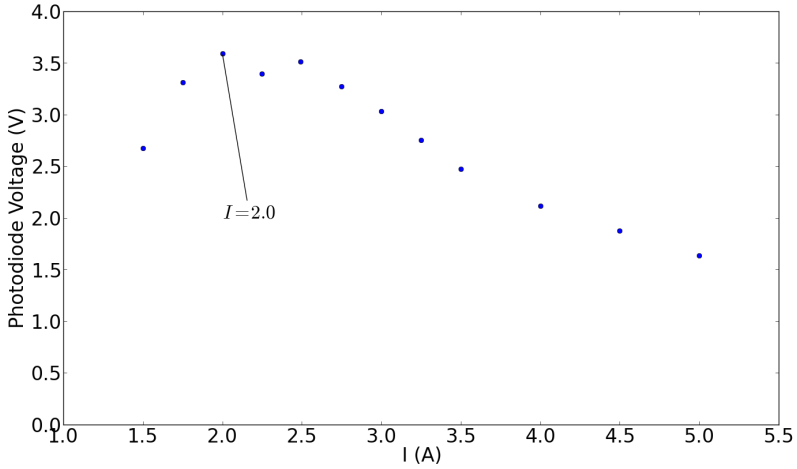

Figure 18: Tuning the 2D MOT coils current for maximum MOT fluorescence.

The parameters are tuned to maximum efficiency by measuring the fluorescence of the MOT with the photodiode. The photodiode output in Volt is depicted on an oscilloscope. The uncertainty in reading out the signal is about 0.5%. The photodiode measures a background fluorescence of 8.24 mV.

First, all the alignment is optimized by tuning the mirrors and lenses to maximum output of the photodiode. The intensity of the cooling and repump beams turned out to have a polarization drift. We were able to bring this down to ± 3 mW by tuning $\lambda/2$ the waveplates in front of the fiber that deliver the laser light to the MOT table. The optimization of the other parameters will be discussed in the following sections. The order in which different values are measured is random, to flatten out drifting of the laser beams.

4.2.1 Magnet Currents

The coils currents are varied by tuning the power supplies manually. The 2D coils currents can be read off up to two decimals, which causes an uncertainty of 0.009 A. The 3D and compensation coils can be read off up to one decimal, causing an uncertainty of 0.09 A.

The current of the 2D MOT was varied between 1.75 and 5.00 A. See Figure 18. The fluorescence of the MOT peaks at ~ 2.0 A.

The current of the 3D MOT was varied between 1 and 20.6 A with $I_{2D} = 3.23$ A. See Figure 19. At 1 A, the magnetic field is too weak to be compensated by the compensation coils but strong enough to affect the strip of atoms in the 2D MOT. This low regime is neglected, because it is not the regime we are interested in. The relevant data starts with a current of 2.5 A. The maximum current the power supply was able to deliver was 20.6 A.

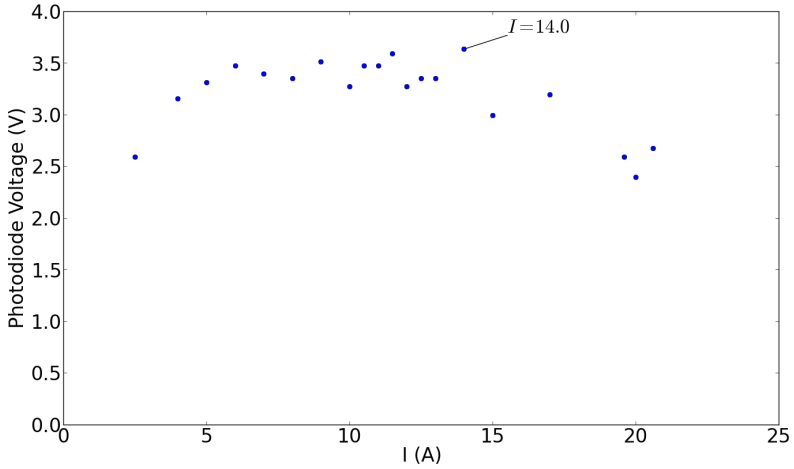

Figure 19: Tuning the 3D MOT coils current for maximum MOT fluorescence with $\delta_{2D} = 0$, $\delta_{3D} = -2.2\gamma$ and $I_{2D} = 3.23$ A.

For a current of 5 - 15 A, the fluorescence of the MOT is flattened and maximal. The data has quite a large spread, probably due to drifting of the lasers. Still, it is clear there is a fairly large 'safe' regime for the 3D MOT currents in which there are no large changes in MOT efficiency. Apparently for $I > 5$ A the magnetic field can not trap atoms more efficiently. And only for $I > 15$ A the atoms are too close (causing them to absorb photons emitted by decaying atoms).

The compensation coils, when varied while keeping the 3D coils current constant at 12 A, show a sharp peak around ~ 1.8 A when varying their current. See Figure 20. This poses no problems, for it only boosts the efficiency of the MOT.

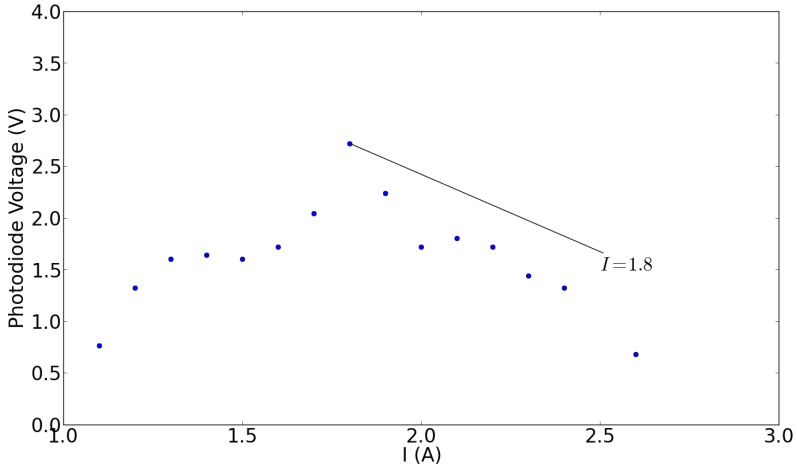

Figure 20: Tuning the compensation coils current for maximum MOT fluorescence with $\delta_{2D} = 0$, $\delta_{3D} = -2.2\gamma$ and $I_{3D} = 12$ A.

4.2.2 Laser Intensity

The push beam intensity is varied by tuning the AOMs. First a rough measurement is made for approximately 0 - 2500 μW, to find the regime of interest. The result is shown in Figure 21.

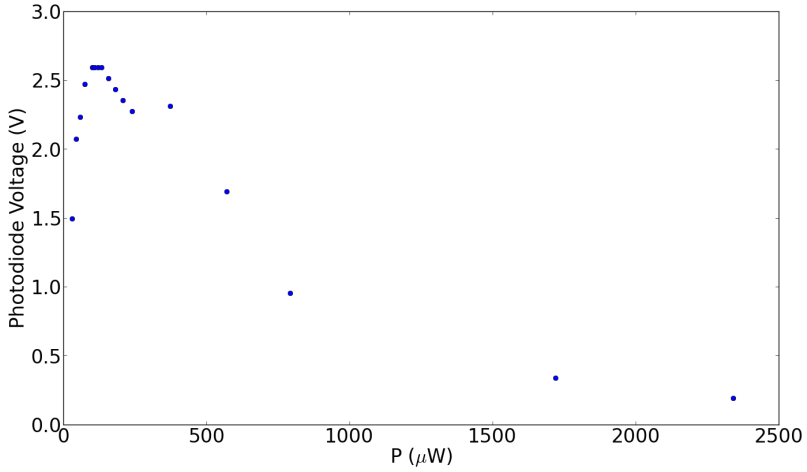

Figure 21: The influence of the push beam intensity over a wide range.

The power of the beam is measured using a power meter. The output was not constant, so the average of 1 minute was used. The uncertainty in reading off the power meter was ± 0.0005 μ W. The fluorescence of the MOT is maximum

for a power of 0 - 500 μW. The values for 0 - 250 W are shown in Figure. For $P \in [100, 140]$ μW the fluorescence is highest.

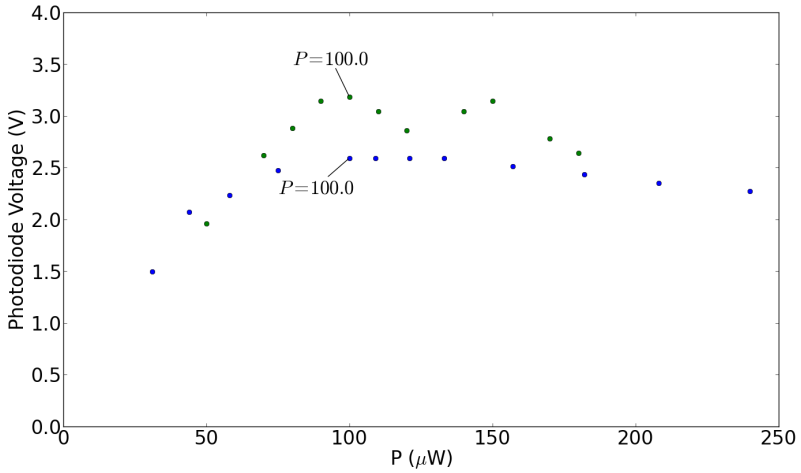

Figure 22: The push beam intensity in the sensitive regime, before (blue) and after (green) the new rubidium ampul was installed. Here $\delta_{2D} = 0$, $\delta_{3D} = -2.2\gamma$, $I_{2D} = 3.7$ A, $I_{3D} = 12$ A and $I_{CC} = 1.8$ A.

After installing a new ampul of rubidium, the fluorescence for $P \in [0, 250]$ μW is measured twice. The average of these measurements is shown in Figure 22. On the whole, the fluorescence has improved due to the new ampul. There are two peaks: $P \sim 100$ μW and $P \sim 150$ μW. Between these peaks the fluorescence slightly decreases. We can conclude the optimum power for the push beam has not shifted significantly.

For the cooling and repump beams it is expected that the intensity is desired to be as large as possible. This is tested for the 2D laser beams, whose intensity is varied by sending a higher current through the diode laser. The fluorescence is measured for $P \in [130, 230]$ mW. See Figure 23. The uncertainty in reading off the power meter for these beams is ± 0.5 mW. As foreseen, the fluorescence improves for increasing intensities. The same is assumed to happen for the 3D cooling and repump beams.

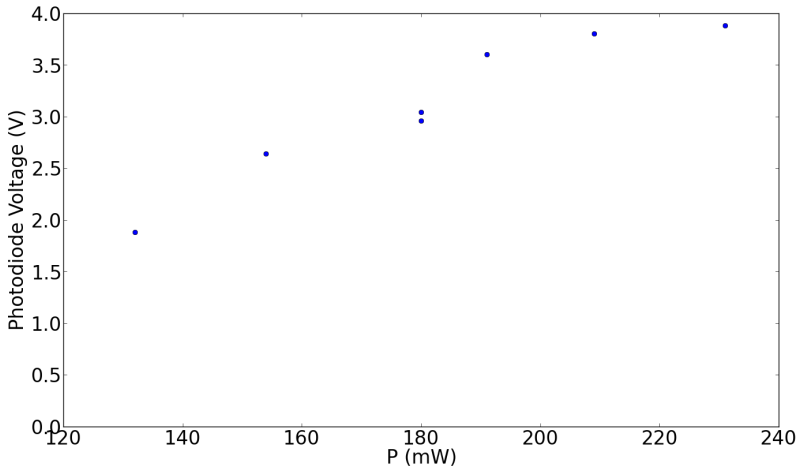

Figure 23: Tuning the 2D cool laser intensity for maximum MOT fluorescence.

4.2.3 Laser Detuning

The detunings of the 2D and 3D cooling beams are varied between -6 and 0 γ using the DDS. The results are shown in Figure 24. The 2D detuning was varied for $\delta_{3D} = -1.8\gamma$. It shows a peak at $\delta_{2D} \sim -3\gamma$.
The 3D detuning was varied for $\delta_{2D} = -2.25\gamma$. The curve is shaped similar to the varied 2D detuning, with a peak at $\delta \sim -1.5\gamma$.

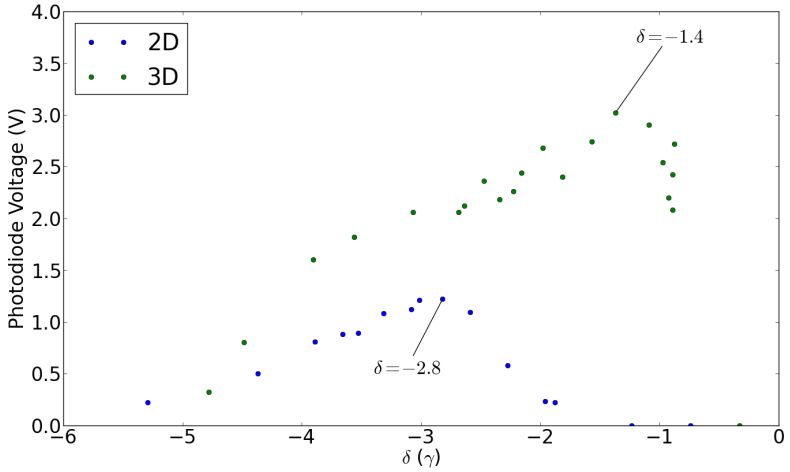

Figure 24: Tuning the 2D MOT frequency with $I_{2D} = 2.8$ A, $I_{3D} = 14.1$ A, $I_{CC} = 1.9$ A, $P_{push} = 0.112$ μW and $\delta_{3D} = -1.8\gamma$. Tuning the 3D MOT frequency with $I_{2D} = 3.2$ A, $I_{3D} = 11.4$ A, $I_{CC} = 1.7$ A and $delta_{2D} = 0$.

5 Conclusion & Discussion

We have succesfully maximized the loading efficiency by tuning several parameters.

To calculate an effective on-resonance saturation parameter s_0, which depends on the intensity of the lasers, we fitted a Lorentzian function to the emission spectrum by varying the detuning. By measuring the fluorescence with a photodiode, we calculated the number of atoms. The maximum number of atoms was $\sim 10^{10}$ for a detuning of $\sim -2\gamma$. This number is easily sufficient for our purposes. We have determined s_0 to be between 10 and 40, improving the earlier estimate of 60.

We varied the magnetic field strength and laser intensities and detunings to optimize the loading rate. The loading rate turns out to be best for $I_{2D} = 2.0$ A, $I_{3D} \in [5, 15]$ A, $I_{CC} = 1.8$ A, $P_{CC} = 100$ μW, maximum intensity for the 2D and 3D cooling and repump lasers, $\delta_{2D} = -2.8\gamma$ and $\delta_{3D} = -1.4\gamma$.

To be able to repeat short measurements automatically, we installed switches. The characteristic time for decay of the currents is in the order of ms. They can be controlled by a computer, giving us the possibility to easily change our loading time.

To control the currents through the coils, it would be useful to control them with a computer. The compensation coils can then be calibrated to the 3D coils optimally. Also, for method (b) the number of atoms look unreliable and not accordance with the results of method (a). This anomaly could be investigated more deeply or the measurements for method (b) could be repeated.

6 Acknowledgements

During my thesis, my enthusiasm for experimental physics has definitely increased. Working with the people from the Cold Atom Nanophotonics group was very pleasant. I would like tot thank Dries van Oosten, Arjon van Lange and Ole Mussmann for supervising my work. Thank you Frits Ditewig, for teaching me how to solder. Also, I want to thank Bas Meyer-Viol, Zimma Kluit, Sebastiaan Greveling, Bruno van Albada and Stephan Wolbers for distracting me with quizzes, lunches, dilemmas and even sometimes help me solving problems for my thesis.

7 References

1. **Citron, M.L., Gray, H.R., Gabel, C.W., Stroud Jr., C.R. (1977, October). Experimental study of power broadening in a two-level atom.** *Physical Review, volume 16.* Retrieved from http://www.optics.rochester.edu/ stroud/publications/citron771.html

2. **Metcalf, H.J. & van der Straten, P. (1999)**. *Laser cooling and trapping.* **New York: Springer-Verlag New York, Inc.**

3. **Pal, S.B. (n.d.)**. *Saturated Absorption Spectroscopy using Rubidium.* **Kolkata: Indian Institute of Science Education & Research**

4. **Steck, D.A.(2001).** *Rubidium 87 D Line Data.* **Oregon: Oregon Center for Optics and Department of Physics, University of Oregon**. Retrieved from http://steck.us/alkalidata (revision 2.0.1, 2 May 2008).

5. **Taylor, J.R. (1997).** *An introduction to error analysis: The study of uncertainties in physical measurements* (2nd edition). **Sausalito, California: University Science Books**

6. **Ellis, Andrew M. (1999). Spectroscopic Selection Rules: The Role of Photon States**. *Journal of Chemical Education, volume 76.* Retrieved from physlab.lums.edu.pk/images/e/ea/AML_paper.pdf.

7. **Henley-Garcia, E. M. (2007)**. *Subatomic Physics.*

8. **Griffiths, D. J. (2005)**. *Introduction To Quantum Mechanics, 2/E.* **Pearson Education India**.

9. **Lett, P., Watts, R., Westbrook, C., Phillips, W., Gould, P., Metcalf, H. (1988). Observation of Atom Laser Cooled Below the Doppler Limit**. *Physical Review, volume 61.*

10. **Lett, P.D., Watts, R.N., Tanner, C.E., Rolston, S.L., Phillips, W.D., Westbrook, C.I. (1989). Optical Molasses.** *The Journal of the Optical Society of America, volume 5.*

11. **Schulz, L. (1999). Sputter-ion pumps.** *CERN European Organization for Nuclear Research Reports, 37-42.* Retrieved from http://www.cientificosaficionados.com/libros/CERN/vacio3-CERN.pdf.

12. **Preston, D. W. (1996). Doppler-free saturated absorption: Laser spectroscopy.** *American Journal of Physics, 64, 1432.* Retrieved from http://ajp.aapt.org.proxy.library.uu.nl/resource/1/ajpias/v64/i11/p1432_s1

13. **Sattar, A. (2003). Insulated Gate Bipolar Transistor (IGBT) Basics.** *IXYS Corporation. IXAN0063.* Retrieved from http://www.ixys.com/Documents/AppNotes/IXYS_IGBT_Basic_I.pdf

14. **Griffiths, D. J., & Reed College. (1999).** *Introduction to electrodynamics (Vol. 3).* **New Jersey: prentice Hall.**

15. **User Guide**. *PDA 36A, Si Switchable Gain Detector*. **Thorlabs, Dachau, Germany**.

A Theory

A.1 Power broadening

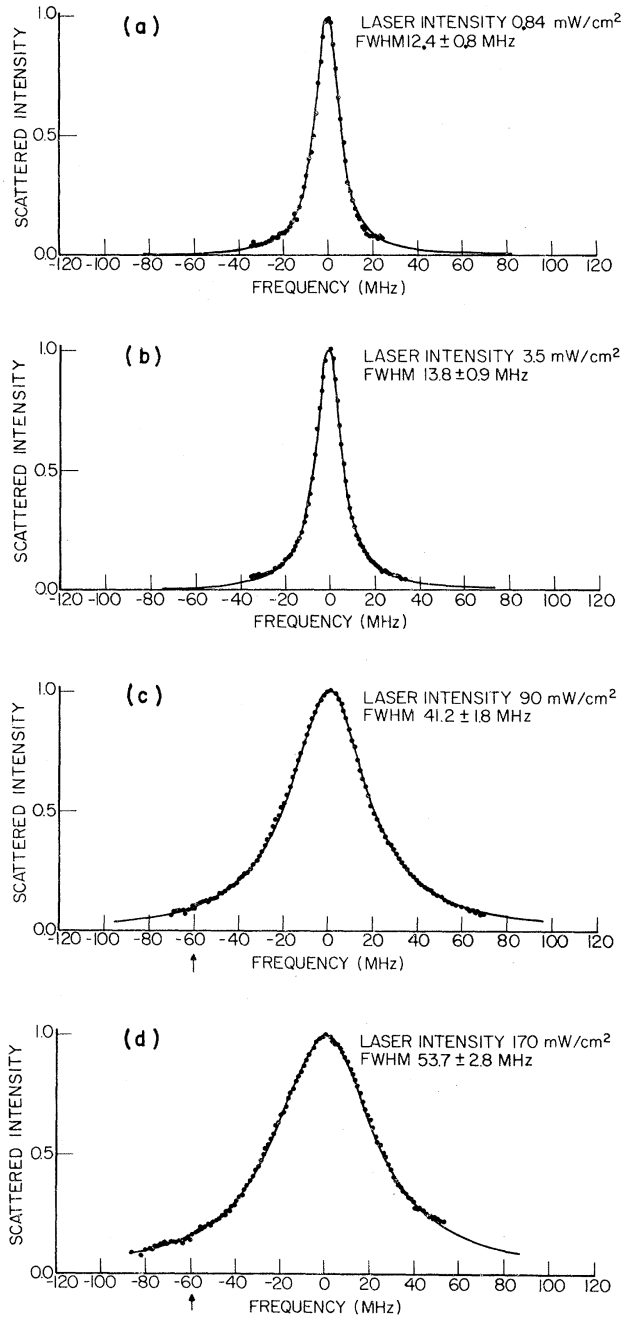

Figure 25: The emission spectra for increased intensities from Citron et al., 1977

A.2 Rubidium Structure

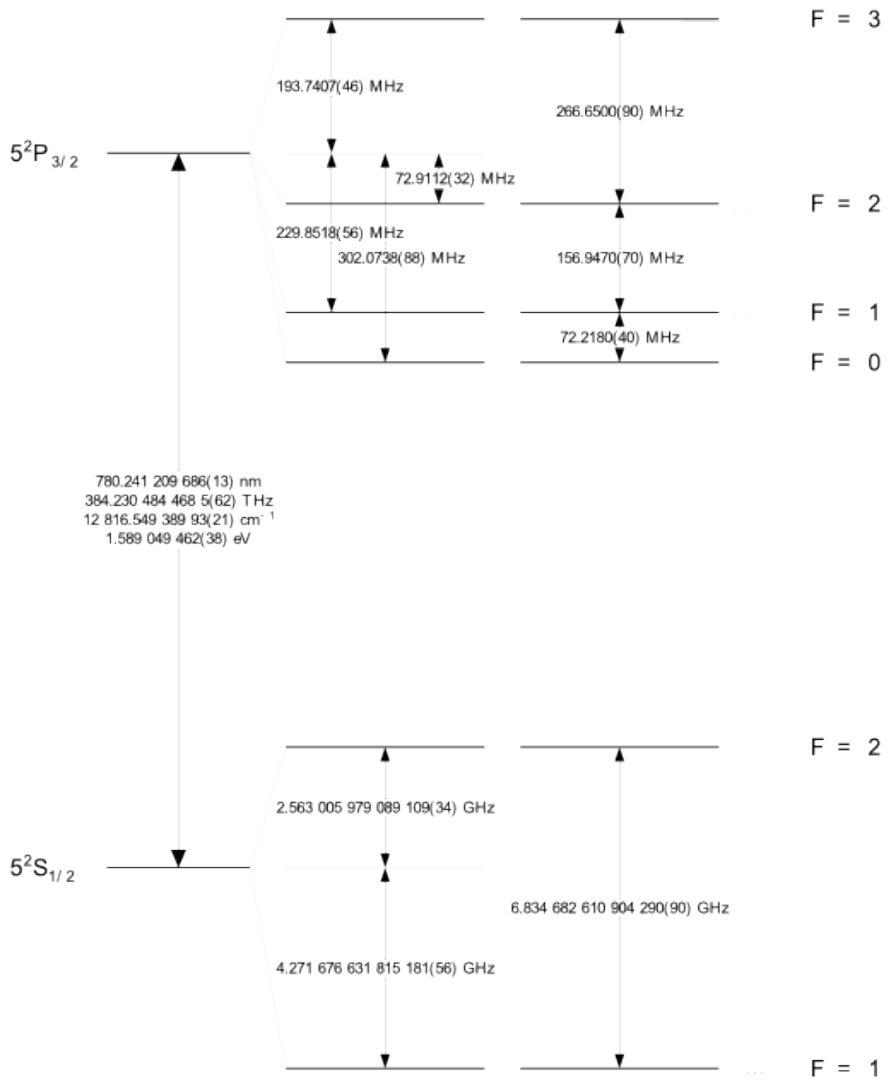

Figure 26: The hyperfine structure for transitions between the fine levels $5^2P_(3/2)$ and $5^2S_(1/2)$, from Steck (2001). These transitions are used to cool the atoms in our MOT.

B Setup

B.1 Compensation Coils

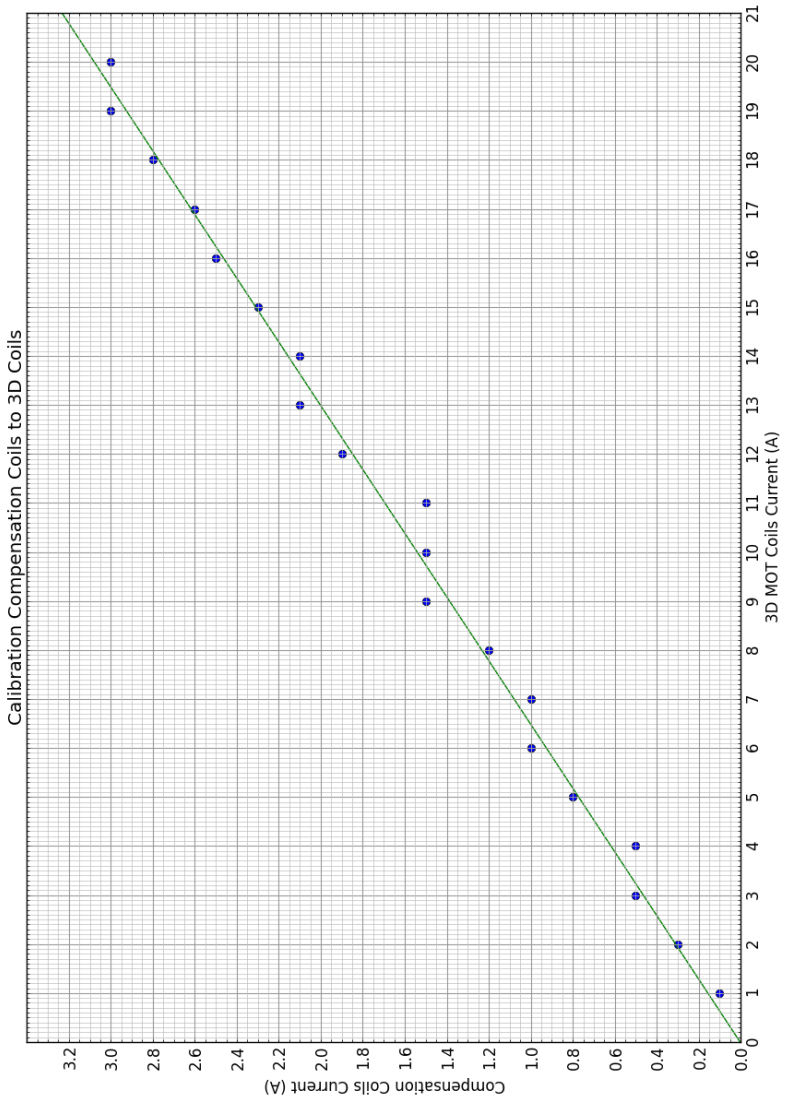

Figure 27: Calibration of the compensation coils current to the 3D MOT coils current.

C Results

C.1 Sweeping to resonance

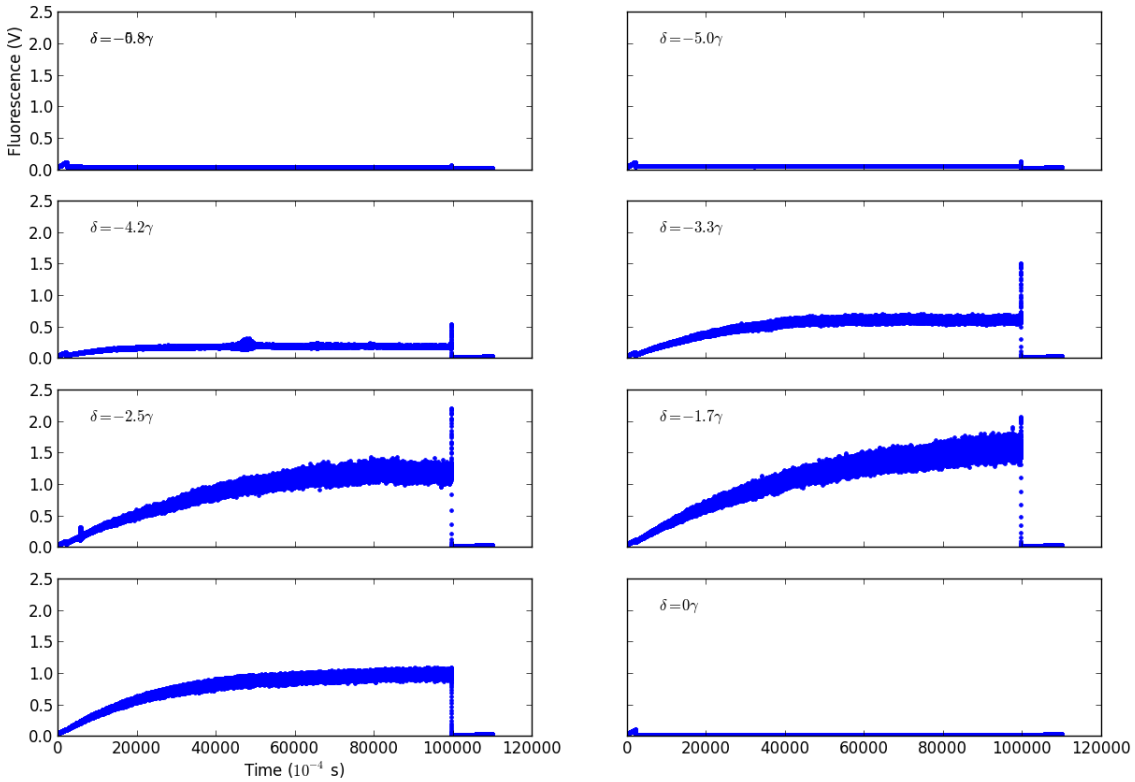

Figure 28: The loading curves obtained using method (a).

C.2 Maximally loading

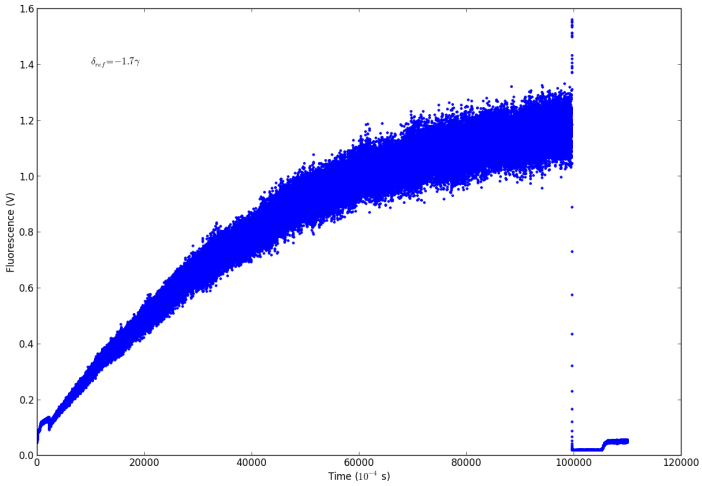

Figure 29: The reference measurement used in method (b).

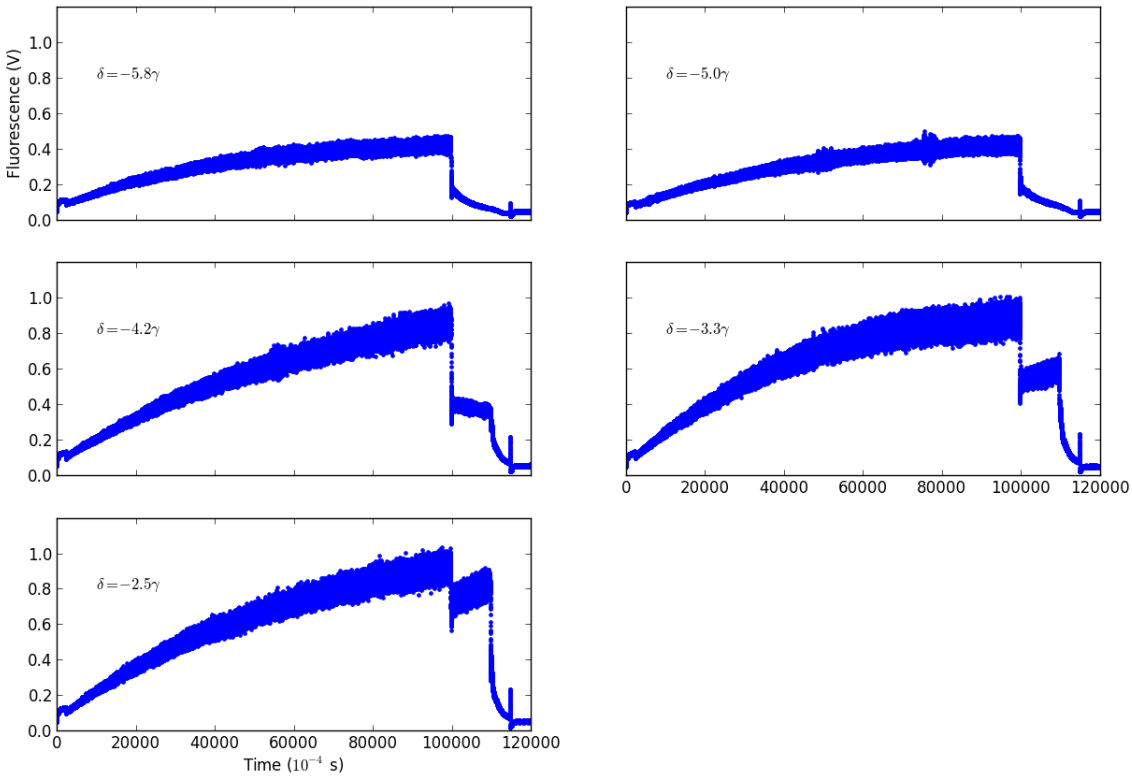

Figure 30: The loading curves obtained using method (b)